

Retention of radioactive methyl iodide in the context of nuclear industry: on the quantification of isotopic exchange contribution inside activated carbons

*Chebbi M *, Lin H *, Monsanglant-Louvet C*, Doizi D ***

*Institut de Radioprotection et de Sûreté Nucléaire (IRSN), PSN-RES/SCA/LECEV, Gif-sur-Yvette, 91192, France

**Commissariat à l'Energie Atomique (CEA), DEN/DES/ISAS/DPC/SECR/LRMO, Gif-sur-Yvette, 91191, France

Abstract:

In this paper, the behavior of TEDA and KI impregnated activated carbons (AC) towards the capture of methyl iodide (CH_3I) is investigated using complementary methodologies. On the one hand, radioactive CH_3I decontamination factors (DF) were determined at different water vapor contents for various commercial activated carbons. A combination between the retention performances and the physico-chemical properties is performed to gain insights about the AC influencing parameters on γ -labelled CH_3I capture. On the other hand, new experimental methodologies are developed in order to measure both stable and γ -labelled CH_3I breakthrough curves (BTC) for KI or TEDA impregnated AC $\{T = 20 - 30 \text{ }^\circ\text{C}$, dry conditions}. These works improve the knowledge about the role played by KI and TEDA. Indeed, TEDA is found to enhance CH_3I retention especially under humid conditions and, for the first time, the KI contribution is isolated and quantified: the KI action towards ^{131}I is highlighted after the breakthrough phase through an isotopic redistribution mechanism.

1 INTRODUCTION

The efficient capture of volatile radioactive iodine species (namely I_2 and CH_3I) potentially released from nuclear facilities remains a very major issue to improve nuclear safety. The specific interest on iodine species stands from their high mobility and their specific affinity for thyroid gland [1,2]. Activated carbons (AC) are employed within the ventilation circuits of nuclear facilities to prevent from volatile iodine dissemination into the environment [3]. These adsorbents display a well-developed microporosity ($d_{\text{pore}} < 2 \text{ nm}$) promoting CH_3I physisorption (kinetic diameter of 0.5-0.6 nm [4]). In the nuclear field, these adsorbents are co-impregnated with triethylenediamine (TEDA, content $\leq 5 \text{ wt.}\%$) and potassium iodide (KI, content about 1 wt.%) in order to ensure a specific and stable storage towards traces of CH_3I as comparison with contaminants present in large excess (namely water vapor) [3]. In addition to the physisorption, different mechanisms are therefore involved for methyl iodide retention by AC. On the one hand, TEDA reacts with CH_3I through chemisorption whose mechanism is reported to be dependent on the relative humidity [5,6]. On the other hand, KI impregnation is associated to an isotopic exchange reaction [7]. Despite the massive and historic use of these adsorbents in the nuclear field, a poor knowledge exists about the most influencing AC parameters towards CH_3I retention efficiency. In addition, uncertainties are persisting about the isotopic exchange mechanism but also on its contribution for total CH_3I uptake under different experimental conditions. Indeed, the postulated retention mechanism due to KI is rarely studied in the literature as a comparison with chemisorption phenomena due to TEDA [5,6]. In the present research work, we aim to bridge these gaps by combining several complex test benches towards CH_3I retention with physico-chemical characterizations of the tested adsorbents. A first part will be dedicated to establish structure-activity relationships between AC intrinsic properties and their retention performances in terms of decontamination factors (DF). Then, a specific attention will be devoted to KI-impregnated AC through breakthrough curves measurements towards both stable and radioactive CH_3I .

2 MATERIALS AND METHODS

2.1 Presentation of the tested adsorbents

Different commercial AC impregnated separately with KI or TEDA are selected for the present study. The theoretical contents in impregnants are reported in Table 2 (see section 3.1.).

2.2 Physico-chemical characterizations

N₂ porosimetry at 77 K completed by H₂O sorption isotherms at 25°C are performed in order to assess the AC available microporosity. Moreover, chemical analyses at different scales are conducted in order to gain insights on {KI, TEDA} quantities and their dispersions within the porous network.

2.3 Experimental setups

Robust and complementary methodologies are developed in order to assess the retention performances towards CH₃I. Decontamination Factors (DF) of radioactive CH₃I are determined through standardized protocols [8,9] in order to assess the role played by KI and TEDA as a function of relative humidity. Moreover, BreakThrough Curves (BTC) are measured towards both stable and radioactive CH₃I through two separate setups to study the temporal evolution of isotopic exchange reaction. Table 1 summarizes the main characteristics and principles of each tested experimental configuration.

Table 1: Main characteristics of the investigated experimental configurations.

	Dynamic adsorption experiments towards CH ₃ ¹²⁷ I	Dynamic adsorption experiments towards CH ₃ ¹²⁷⁺¹³¹ I (γ-labelled CH ₃ I)	
Objective	<u>BTC curves</u>	<u>DF determination</u>	<u>BTC curves</u>
AC conditioning	Grain size selection between 1 and 1.4 mm <i>Ex-situ</i> pretreatment at 100°C overnight Mass of about 10 g	Grain size between 2 and 3 mm Pre-equilibration under flowing water vapor for at least 16 hours (T = 20°C, RH = 40% or 90%) Mass of 35-40 g	Grain size selection between 1 and 1.4 mm <i>Ex-situ</i> pretreatment at 100°C overnight Mass of about 10 g
Principle	Continuous injection of CH ₃ I from a certified bottle up to the AC saturation	Pulse injection of radioactive CH ₃ I (30 min) followed by an elution under air (1h)	Continuous injection of radioactive CH ₃ I (certified bottle + permeation tube) up to the AC saturation
Flow conditions	C = 10 ppmv, T = 30°C, RH = 0% v = 25 cm/s, residence time = 0.2 s	C = 0.6 ppmv, ¹³¹ I activity : 62 kBq (RH=90%) or 617 kBq (RH=40%) T = 20°C, RH = 40% or 90% v = 25 cm/s, residence time = 0.2 s	C = 10 ppmv, ¹³¹ I flowrate = 150 Bq/min T = 20°C, RH = 0% v = 25 cm/s, residence time = 0.2 s
Detection method	Online measurement by Gas Chromatography coupled with a Pulsed Discharge Electron Capture Detector (PD-ECD)	<i>Ex-situ</i> measurement by γ-spectrometry at the end of test	Continuous sampling and <i>ex-situ</i> measurement by γ-spectrometry up to the AC saturation

3 RESULTS AND DISCUSSIONS

3.1 Main properties of the investigated adsorbents

According to XRD and SEM/EDX analyses, TEDA and KI molecules were found during our previous study [10] to be well dispersed within the internal porosity without clusters formation on the external surface. The presence of these species may alter the accessible microporosity to CH₃I physisorption. Hence, a peculiar attention is devoted to the textural properties of the tested materials as deduced mainly from N₂ porosimetry at 77 K (Table 2). Generally, high specific surface areas (around 1000 m²/g) are obtained, with an important contribution due to the micropores (> 94%), in line with developed AC for the nuclear field [11]. A closer look to the data reported in Table 2 indicates a different behavior depending on the impregnation

nature. KI/AC display a rather similar microporosity due to their low KI content (< 0.4 % in molar, Table 2). However, a decreasing evolution can be noticed for S_{BET} and V_{micro} for TEDA/AC, especially after 3 wt.% in TEDA (Table 2). This partial micropore blocking may be assigned to the presence of TEDA entities within or in the micropores openings, consistently with XRD and SEM/EDX analyses [10]. N_2 porosimetry analyses are completed by H_2O adsorption isotherms at 25°C in order to better assess the influence of water vapor on the starting adsorbents before exposure to CH_3I (DF measurements, section 3.2). At low RH, the water uptake is found to increase with KI content, due to the nucleation effect [10,12]. In contrast, TEDA impregnated AC are less sensitive to water molecules as a comparison with KI/AC [10]. At high RH, the water uptake is rather dependent on the AC microporosity in agreement with former works [12].

Table 2: Textural properties of the tested adsorbents as deduced by N_2 porosimetry at 77 K.

AC designation	Molar ratio (%)	S_{BET} (m ² /g)	V_{micro} (cm ³ /g)	AC designation	Molar ratio (%)	S_{BET} (m ² /g)	V_{micro} (cm ³ /g)
Non-impregnated (NI)	0	1142 ± 67	0.453 ± 0.031	Non-impregnated (NI)	0	1142 ± 67	0.453 ± 0.031
<u>0.1%</u> KI/AC	0.007	1174 ± 67	0.469 ± 0.026	<u>1%</u> TEDA/AC	0.107	1217 ± 90	0.489 ± 0.043
<u>0.5%</u> KI/AC	0.036	1171 ± 154	0.470 ± 0.066	<u>3%</u> TEDA/AC	0.321	1097 ± 59	0.441 ± 0.028
<u>1%</u> KI/AC	0.072	1213 ± 134	0.486 ± 0.058	<u>5%</u> TEDA/AC	0.535	1022 ± 31	0.410 ± 0.012
<u>2%</u> KI/AC	0.145	1174 ± 0	0.469 ± 0.002	<u>7%</u> TEDA/AC	0.749	938 ± 90	0.380 ± 0.035
<u>5%</u> KI/AC	0.361	1132 ± 69	0.456 ± 0.032	<u>10%</u> TEDA/AC	1.070	824 ± 146	0.332 ± 0.059

* The reported percentage is related to the theoretical massic content for KI or TEDA.

3.2 γ -labelled CH_3I DF measurements

The obtained performances for TEDA and KI impregnated AC as a function of relative humidity (T = 20°C) according to the reported methodology in Table 1 are presented in Figure 1.

3.2.1 T = 20°C, RH = 40%

Different features can be highlighted as a function of the molecule nature. For TEDA/AC, an enhancement of DF is observed first from (106 286 ± 35 606) to (220 228 ± 46 423) for increasing TEDA contents from 1 to 5 wt.% (Figure 1 (A)), then a slight decrease in DF can be noticed when using higher TEDA contents (Figure 1 (A)). This behavior is explained by the occurrence of two opposite mechanisms for CH_3I trapping : physisorption and chemisorption. The first one is dependent on the available microporosity which decreases after TEDA incorporation (Table 2). The second mechanism is driven by an alkylation mechanism in moderately humid conditions [6]. From DF evolution as a function of the available microporosity (Figure 1 (A)), the compromise between these two mechanisms seems to be a TEDA content of 5 wt.%.

However, lower retention performances are outlined for KI/AC. A paradoxical decrease of DF is even observed as a function of KI content from (10 917 ± 4 981) for non-impregnated AC to (236 ± 29) for 5 wt.% KI AC (Figure 1 (A)). It seems that the behavior of KI/AC at this set of condition is dominated by physisorption rather than isotopic exchange as evidenced from the increasing evolution of DF versus the available microporosity for these adsorbents (Figure 1 (A)). The absence of compromise between KI content and accessible microporosity, as observed with TEDA/AC, may indicate in other words the absence of isotopic exchange under the studied conditions {T=20°C, RH=40%}.

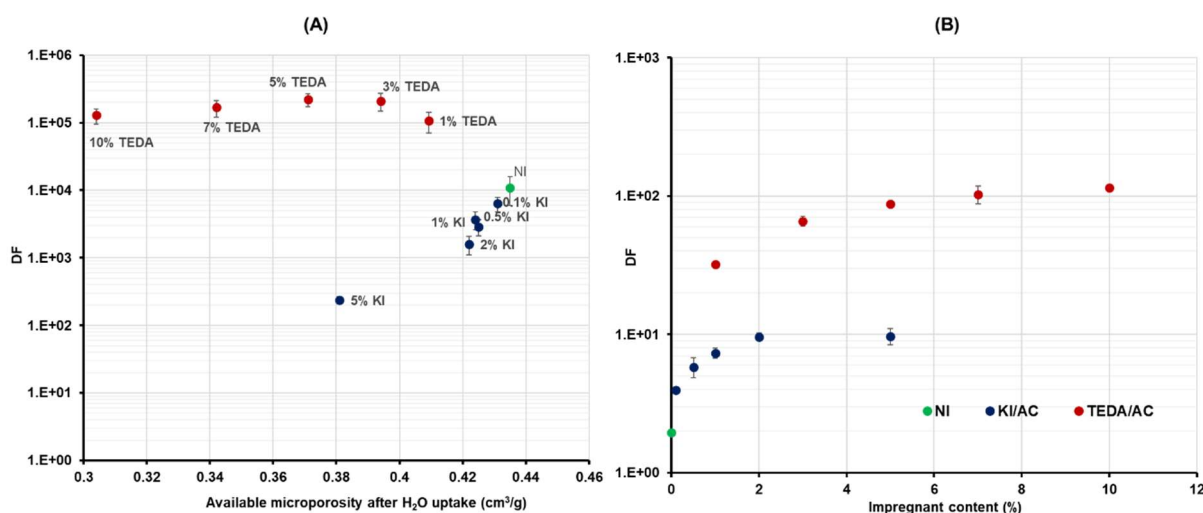


Figure 1: (A) Evolution of CH₃I retention performances for TEDA and KI impregnated AC as a function of the available microporosity calculated from N₂ porosimetry and H₂O adsorption isotherms at {T = 20°C, RH = 40%}. (B) Evolution of CH₃I retention performances as a function of the impregnant content at {T = 20°C, RH = 90%}.

3.2.2 T = 20°C, RH = 90%

At the second set of conditions, a drastic decrease of DF is observed for AC. This detrimental effect can be overcome especially thanks to TEDA impregnation. Indeed, a DF increase from (32 ± 5.8) to (103 ± 4.6) can be noticed for TEDA loadings of 1 wt.% and 7 wt.% respectively, followed by a less pronounced enhancement at TEDA content of 10 wt.% (DF = (115 ± 5.9), Figure 1 (B)). Considering the same conditions, a beneficial role due to KI impregnation can also be highlighted with a slight increase of DF from (1.96 ± 0.08) to (9.71 ± 0.87) (Figure 1 (B)).

To sum-up, the physisorption contribution is significantly reduced at RH = 90%. The DF increase with both TEDA and KI impregnations is therefore assigned to chemisorption and isotopic exchange respectively. Nevertheless, the extent of DF increase due to KI impregnation is less important as a comparison with TEDA, owing to its high reactivity through a protonation mechanism as proposed in the literature [6].

3.2.3 Discussions about isotopic exchange occurrence

Using the normalized procedures for DF determination, the isotopic exchange reaction *via* KI seems to be observed only under humid conditions. According to a previous work [13], the isotopic exchange effect was only evidenced during the breakthrough phase. At RH=40%, the KI/AC are still in the retention phase due to high obtained DF values. However, the low performances at RH=90% indicate the AC breakthrough, which explains the observation of this reaction only at humid conditions. Nevertheless, a slight contribution from this mechanism can be highlighted using the normalized protocol as a comparison with TEDA. The next section will be devoted to describe the results obtained with KI using BTC for both stable and radioactive CH₃I in order to better assess this reactivity.

3.3 Breakthrough curves towards stable and γ -labelled CH₃I

The obtained CH₃I sorption profiles for KI/AC are presented in Figure 2. A comparison with TEDA/AC for the capture of stable CH₃I is also provided in Figure 2 (A).

3.3.1 Stable CH₃I breakthrough curves

First, the investigation of KI/AC behavior towards stable CH₃I (T=30°C, HR=0%) indicates as expected the occurrence of only physisorption, which is dependent on the microporosity accessibility by the adsorbate [14]. Indeed, similar performances are observed for KI/AC (retention phase duration of about 5 hours, Figure 2 (A)) in agreement with their similar microporosity (Table 2). A significant improvement of stable CH₃I retention performances can be outlined after TEDA incorporation (5 wt.%), with a retention phase duration of 12 hours (Figure 2 (A)). This enhancement is assigned to the occurrence of chemisorption phenomena resulting in a strong storage of CH₃I molecules in agreement with our previous batch reactor study [14].

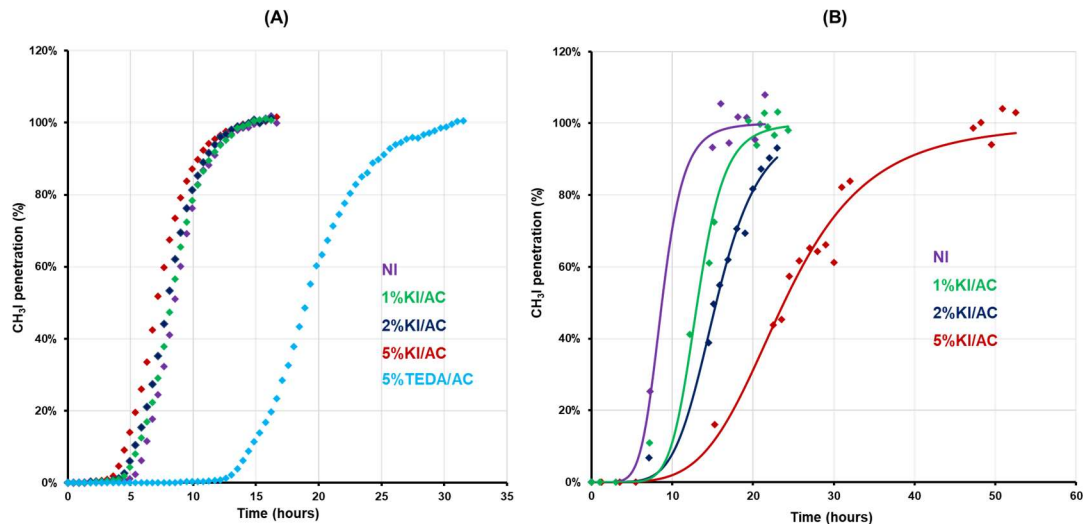


Figure 2: (A) Influence of KI and TEDA impregnations on stable CH₃I BTC at {T = 30°C, RH = 0%}. (B) Radioactive CH₃I BTC over KI-impregnated AC at {T = 20°C, RH = 0%}. The fitted curves according to an improved Thomas model are presented in lines for γ -CH₃I.

3.3.2 Radioactive CH₃I breakthrough curves

Using the methodology summarized in section 2.3. (Table 1), the obtained BTC for KI/AC towards γ -CH₃I are presented in Figure 2 (B), with the corresponding fitted curves of the improved Thomas model [15]. Firstly, no significant change in the retention phase duration (around 5 h, Figure 2 (B)) is observed for γ -labelled CH₃I adsorption as a comparison with stable CH₃I (Figure 2 (A)). Considering the breakthrough phase, a progressive improvement of AC performances towards γ -CH₃I can be noticed, with an enhancement of saturation time from 14 h (non impregnated AC) to about 46 h for 5%KI/AC (Figure 2 (B)). This behavior is due to the isotopic exchange reaction between ¹²⁷I (from KI) and ¹³¹I (from γ -labelled CH₃I) [7,13], owing to the similar performances towards stable and γ -CH₃I for non-impregnated AC and TEDA/AC. This isotopic redistribution seems to be more significant during the breakthrough phase, in line with assumptions presented previously (section 3.2.3).

3.3.3 Quantification of the relative contribution due to isotopic exchange

For the first time, we are able to isolate the isotopic exchange phenomena. Two preliminary attempts to quantify this reaction are also performed. On the one hand, the relative contribution due to this mechanism can be expressed in terms of the time delay to reach the AC total saturation (penetration of 100%) towards γ -CH₃I as a comparison with stable CH₃I. An increasing relative contribution is therefore calculated from 39% (1%KI/AC) to 70% (5%KI/AC). On the other hand, a more generalized expression of this contribution as a function of γ -CH₃I penetration has been established for the first time in order to better evaluate the importance of this reaction in the AC working range within nuclear facilities (maximal penetrations of about 1-10%). More precisely, the extrapolation to a penetration of 1% through the use of an improved Thomas model for both stable and radioactive CH₃I sorption profiles, has allowed to estimate a relative contribution of about 19% for 5%KI/AC. These first calculations highlight the importance of the isotopic exchange reaction from CH₃I low penetrations.

4 SUMMARY

In this paper, we have presented recent research and development works about CH₃I adsorption by TEDA or KI impregnated AC through complementary methodologies (DF measurements and BTC for both stable and radioactive CH₃I). For the first time, the contribution due to KI, still rarely studied in the literature, is isolated from the other dominant mechanisms (physisorption and chemisorption). A first quantification of the reactivity due to KI is also provided. This attempt highlights the important effect of isotopic exchange for the retention of radioactive CH₃I. Some technical improvements are nevertheless required about BTC acquisition towards radioactive CH₃I, to ensure a more accurate quantification of this reactivity at low penetrations and depending on the experimental conditions (T, R.H.). From a phenomenological point of view, we have also made significant progress to unravel the

relationships between KI, TEDA impregnants and the associated CH₃I sorption profiles. On the one hand, the high affinity of TEDA for CH₃I leads to the retention phase duration increase accompanied by DF enhancement and trapping stability improvement. A such reactivity is required to retain CH₃I with good efficiency especially under stringent conditions (high temperature and humid conditions). On the other hand, KI action seems to be evidenced after the breakthrough phase allowing to slow down the desorption of physisorbed radioactive CH₃I. This reaction seems to be kinetically unfavored as a comparison with chemisorption or physisorption. This reactivity may play nevertheless a crucial role to prevent from an early AC filter replacement because of ageing phenomena.

Further studies will be performed during our research team with the aim to finely quantify the contribution due to isotopic exchange. The challenge is to identify new synthesis strategies promoting this reaction before its kinetic modelling under various experimental conditions. These aspects are crucial towards the development of a novel non-radioactive methodology for iodine traps periodic test to limit the radioactive discharges into the environment because of conventional radioactive methods.

5 REFERENCES

- [1] B. Clément, L. Cantrel, G. Ducros, F. Funke, L. Herranz, A. Rydl, G. Weber, C. Wren, "State of the art report on iodine chemistry," NEA/CSNI/R(2007)1, 2007.
- [2] D.R. Haefner, T.J. Tranter, "Methods of Gas Phase Capture of Iodine from Fuel Reprocessing Off-Gas: A Literature Survey," Idaho National Laboratory, 2007 INL/EXT-07-12299.
- [3] J. Huve, A. Ryzhikov, H. Nouali, V. Lalia, G. Augé, T. J. Daou, RSC Adv. 8 (2018) 29248.
- [4] R.D. Scheele, L.L. Burger, C.L. Matsuzaki, "Methyl Iodide Sorption by Reduced Silver Mordenite," Pacific Northwest Laboratory, 1983 PNL-4489 .
- [5] K. Ho, S. Moon, H.C. Lee, Y.K. Hwang, C.H. Lee, J. Hazard. Mater. 368 (2019) 550.
- [6] K. Ho, H. Chun, H.C. Lee, Y. Lee, S. Lee, H. Jung, B. Han, C.H. Lee, Chem. Eng. J. 373 (2019) 1003.
- [7] F. Kepák, J. Radioanal. Nucl. Chem. 142 (1990) 215.
- [8] " NF M62-206, Méthode de contrôle du coefficient d'épuration des pièges à iode," 1984.
- [9] " ASTM D3803-91(2014), Standard Test Method for Nuclear-Grade Activated Carbon," 2014.
- [10] H. Lin, M. Chebbi, C. Monsanglant-Louvet, B. Marcillaud, A. Roynette, D. Doizi, P. Parent, C. Laffon, O. Grauby, D. Ferry, J. Hazard. Mater. 431 (2022) 128548.
- [11] C. M. González-García, J. F. González, S. Román, Fuel Process. Technol. 92 (2011) 247–252.
- [12] D. D. Do, H. D. Do, Carbon 38 (2000) 767–773.
- [13] G. O. Wood, F. O. Valdez, "Nonradiometric and radiometric testing of radioiodine sorbents using methyl iodide," in Proceedings of the 16th DOE Nuclear Air Cleaning Conference, 1980.
- [14] M. Chebbi, C. Monsanglant-Louvet, P. Parent, C. Gerente, L. Le Coq, B. M. Mokili, Carbon Trends 7 (2022) 100164.
- [15] R. Apiratikul, K. H. Chu, J. Water. Process. Eng. 40 (2021) 101810.